Electrocatalysis

DOI: 10.1002/ange.201205354

# The Role of Catalysts and Peroxide Oxidation in Lithium–Oxygen Batteries**

*Robert Black, Jin-Hyon Lee, Brian Adams, Charles A. Mims, and Linda F. Nazar**

*Dedicated to Professor John B. Goodenough on the occasion of his 90th birthday*

Much attention has been devoted recently to rechargeable lithium–oxygen batteries because of their very high energy density compared to that of other rechargeable systems.[1] Theoretically, it can reach up to 2–3 kWh kg$^{-1}$ with respect to the mass of the discharged electrode, although practical values are expected to be in the range of 1000 Wh kg$^{-1}$. However, high overpotential on charge that results in poor round-trip efficiency, along with poor cyclability makes the use of Li-$O_2$ batteries impractical until these problems are solved.[2] Various catalysts have been examined to lower the activation barriers, such as nanowire α-$MnO_2$, $Co_3O_4$, $Mn_3O_4$, and PtAu, with many studies having been conducted in alkyl carbonate electrolytes.[3–5] Spinel-based $M_3O_4$ (M = Mn,Co) catalysts supported on graphene were reported to be promising bifunctional catalysts in aqueous media.[6,7] However, these electrolyte systems do not rely on $Li_2O_2$ formation and its subsequent OER as would be the case in an aprotic Li-$O_2$ cell. Moreover, some recent articles question the efficacy or necessity of catalysis in the aprotic system.[8] Our studies were aimed at addressing this. Here, we show that nanocrystalline $Co_3O_4$, grown on reduced graphene oxide ($Co_3O_4$/RGO) and employed as part of a carbon-based oxygen electrode membrane, results in significant reduction of overpotentials for OER (up to 350 mV), and improved cycling performance. The material acts as a promoter, rather than as a classic electron-transfer catalyst for the reactions involved in the Li-$O_2$ cell.

The synthesis of $Co_3O_4$/RGO was carried out by reduction of cobalt phthalocynanine deposited onto graphene,[9] followed by mild oxidation (see the Supporting Information). Figure 1 shows the X-ray diffraction (XRD) pattern of the material and a representative high-resolution transmission electron microscopy (HRTEM) image. The XRD reflections index to the cubic spinel, $Co_3O_4$ (Figure 1a). The absence of graphene oxide peaks proves that the carbon sheets are in a substantially exfoliated state, and do not restack during the reduction and oxidation processes. The HRTEM image (Figure 1b) reveals that 8–10 nm $Co_3O_4$ particles litter the surface of the graphene sheets (also shown in the low-resolution TEM in Figure S1 in the Supporting Information). The selective area electron diffraction (SAED) pattern further confirms nanocrystalline $Co_3O_4$ with a cubic spinel structure. Since some graphene/graphene oxides have been shown to be quite effective for ORR,[10] a high metal oxide content (55 wt%; see Figure S2) was deliberately chosen so that the $Co_3O_4$ nanocrystals cover all of the graphene oxide surface (see Figure 1b). This permits the properties of the oxide catalyst to be investigated independently, since graphene acts primarily as a conductive layer to support the high metal oxide dispersion.

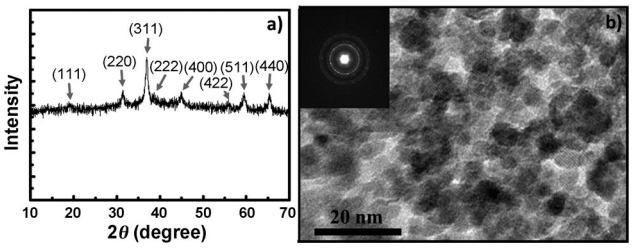


***Figure 1.*** $Co_3O_4$/RGO: a) XRD pattern, cubic spinel reflections indicated. b) HRTEM image, inset: SAED pattern of $Co_3O_4$.

The electrochemical performance of Li-$O_2$ cells using a 1M $LiPF_6$/tetraethylene glycol dimethyl ether (TEGDME) electrolyte—constructed with cathodes comprised of either $Co_3O_4$/RGO mixed with 70% Ketjen black (KB), or KB alone—is shown in Figure 2. Electrodes without KB failed to exhibit significant discharge capacity (five were sampled for reproducibility), indicating that the $Co_3O_4$/GO itself is inactive for ORR. In Figure 2a, the initial discharge–charge curve for $Co_3O_4$/GO/KB is compared to KB. Both cells exhibited similar high capacities of between 12000–14000 mAh $g_c^{-1}$ ($g_c$ = gram carbon) on full discharge. XRD analysis of discharged electrodes (Figure 2b) demonstrates that $Li_2O_2$ is the only crystalline product in both cases, with dimensions between 18–20 nm based on Scherrer analysis. Nucleation and aggregation of the $Li_2O_2$ nanocrystallites results in "toroids" that are relatively uniform in size, as previously reported.[11,12]

[*] Prof. L. F. Nazar
Department of Chemistry
and the Waterloo Institute for Nanotechnology
University of Waterloo
200 University Ave W., Waterloo Ontario (Canada)
E-mail: lfnazar@uwaterloo.ca
R. Black, J.-H. Lee, B. Adams
Department of Chemistry
University of Waterloo (Canada)
Prof. C. A. Mims
Department of Chemical Engineering
University of Toronto
200 St. George Street, Toronto Ontario (Canada)

[**] We thank the NSERC for financial support through its discovery and strategic grant programs.

Supporting information for this article is available on the WWW under http://dx.doi.org/10.1002/anie.201205354.

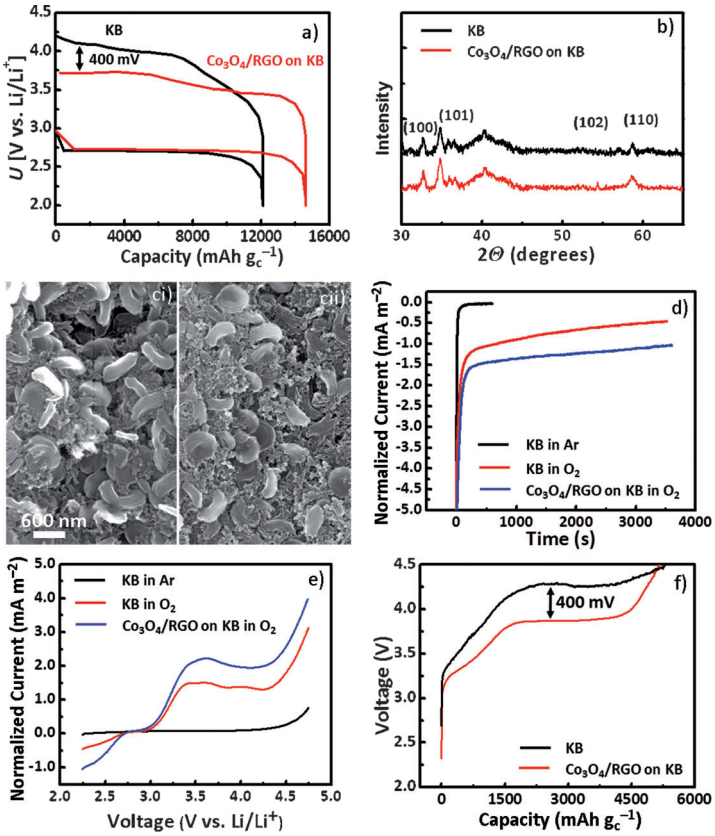


***Figure 2.*** a) First discharge–charge profile for Li-$O_2$ cells with Ketjen black (KB) or $Co_3O_4$/RGO/KB at 25 °C at a current rate of 140 mA $g^{-1}$. b) XRD patterns of the cells in (a) on first discharge. Reflections of $Li_2O_2$ are marked. c) SEM micrographs of the discharged electrodes at 6000 mAh $g_C^{-1}$: ci) $Co_3O_4$/RGO/KB and cii) KB. d) Chronoamperometry showing normalized current evolution with time at 2.25 V. e) Linear sweep voltammetry following a hold at 2.25 V for 1 h. f) Voltage profile on charge for cells containing chemically deposited $Li_2O_2$ in the presence of either $Co_3O_4$/RGO/KB or KB.

There is no difference in morphology between the toroids produced in the presence or absence of the $Co_3O_4$/GO (Figure 2c). This further indicates that the carbon cathode component is primarily responsible for the reduction of oxygen to $Li_2O_2$. However, there is a 20 mV decrease in the OR overpotential for the $Co_3O_4$/GO cell and a 15% higher capacity. This cannot be explained by an increase in electronic conductivity since the values are similar for both materials (see the Supporting Information).

A thin layer of the electrode materials deposited on a glass carbon electrode was investigated by chronoamperommetry and linear sweep voltammetry (LSV). On holding a constant potential of 2.25 V—below the equilibrium reduction potential of $O_2$—for 1 h (Figure 2d), the current response of $Co_3O_4$/GO/KB is doubled compared to that of KB alone. This demonstrates an enhancement of the kinetics associated with the reduction of $O_2$ to $O_2^-$. Given the small amount of $Co_3O_4$/RGO added to KB (30 wt%), and its comparatively low surface area, the difference in ORR performance cannot be attributed to the surface site population. LSV studies were conducted by first holding the voltage at 2.25 V for 1 h to deposit $Li_2O_2$, and sweeping the voltage up to 4.7 V. The results shown in Figure 2e also indicate a much higher current response with incorporation of $Co_3O_4$/RGO, in part because more peroxide is deposited during the 1 h hold owing to better kinetics. Significantly, the onset of the OER is similar for both KB and $Co_3O_4$/RGO: just above 3.0 V (as expected for the oxide). This is a sharp contrast to the OER in aqueous media, and confirmed by our results (Figure S3) where $Co_3O_4$/graphene acts as a conventional electrocatalyst to significantly lower the onset potential.[7] Our findings are in accord with reports on the efficacy of electrocatalysis in aprotic media, where the role of the catalyst has been queried,[8] and—as in our LSV experiment—a small amount of $Li_2O_2$ was deposited (smaller than about 500 mAh $g^{-1}$). In short, at low levels of peroxide deposition when it is in intimate contact with the carbon material, OER occurs at a similar potential irrespective of the metal oxide.

In contrast, in practical cells where $Li_2O_2$ deposition is substantial (that is, over 2000 mAh $g^{-1}$), the $Co_3O_4$/GO material has a significant effect on the OE. On the first cycle (Figure 2a), the charged electrode with the hybrid catalyst exhibits a charge plateau between 3.5–3.75 V, about 400 mV lower than that of the pure KB carbon electrode (Figure 2a). The reduction in the charge potential for the hybrid catalyst is in keeping with the properties of the metal oxide as first reported.[1] It is also supported by our studies that employ $Li_2O_2$ deposited onto a support from a $KO_2$/$LiPF_6$ solution.[11] Here, the artificially "discharged" electrode is subjected to electrochemical oxidation in a cell. This avoids complications from possible electrolyte decomposition during a prolonged electrochemical reaction. Figure 2f shows that a similar reduction in the OE potential of about 400 mV is obtained for the oxidation of peroxide chemically deposited on $Co_3O_4$/RGO/KB versus KB alone, as observed in the discharge–charge profile shown in Figure 2a.

The overall results described in Figure 2 suggest that $Co_3O_4$/RGO does not act as conventional electrocatalyst to lower the activation energy through electron transfer. Rather, our data indicates that it acts as a promoter to enhance surface transport of $Li_xO_2$ species, by reducing their binding energy in both the forward and reverse electrochemical processes. We base our supposition on two factors. Studies on alkene oxidation reactions demonstrate the presence of mobile surface oxygen species (superoxide and peroxide) on 14–15 nm nanocrystallites of $Co_3O_4$ supported on $CeO_{2-x}$.[11] The second is our prior finding that $Li_2O_2$ produced on disproportionation of superoxide ($2LiO_2 \rightarrow Li_2O_2 + O_2$) from solution onto high surface area carbon is much less crystalline than in the absence of carbon.[11] We attribute this to the strong binding of superoxide with carbon defect sites that inhibits the disproportionation reaction. Because metal oxide surfaces are considered to be less "sticky" than carbon surfaces riddled with dangling bonds, they could facilitate mass transport of $Li_xO_2$ species. These factors are particularly critical at high capacity where transport becomes limiting. We note that the possible role of the "catalyst" in promoting mass

transport was recently put forward in a slightly different context.[8]

The question is how can the promoter have an effect on the OER, given the large (about 500–700 nm) toroidal aggregates that are formed on discharge. A clue is provided from examination of the full first cycle process for the $Co_3O_4$/RGO electrode, using SEM in combination with analytical studies using XRD, Raman spectroscopy, and time-of-flight secondary-ion mass spectrometry (ToFSIMS). The $Li_2O_2$ toroids that are deposited on the surface on discharge to 6000 mAh $g^{-1}$ (point D in Figure 3a) immediately start to disintegrate on oxidation by only 10% (point C1 in Figure 3a). The SEM image corresponds to the point on the

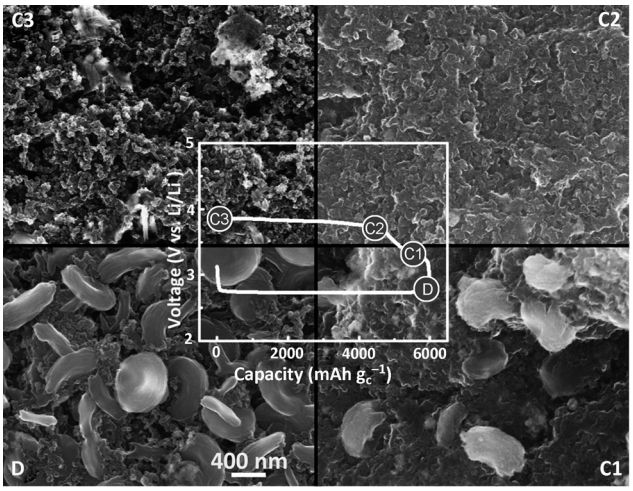


***Figure 3.*** SEM micrographs of the $Co_3O_4$/RGO/KB Li-$O_2$ electrodes taken at the points indicated on the discharge–charge profile (central inset).

charging curve on the first plateau at 3.3 V. This discrete onset potential that we observe is the same as that reported elsewhere for $O_2$ release.[8] Remnants of the nanocrystalline $Li_2O_2$ toroidal aggregrates are still visible, but many have collapsed and filled in the voids between the electrode particles. The SEM image on completion of the transition (at a charge of 25% or 1500 mAh $g^{-1}$ at point C2), shows that the disintegrated toroids form an agglomerate film that covers the electrode surface. This material is amorphous by XRD analysis, and the Raman spectra also show no distinctive spectral features. We propose that surface transport of $Li_xO_2$ species on OER is now facilitated by close proximity to $Co_3O_4$/RGO within the electrode. The majority of the subsequent oxidation (75% of the total charge) takes place at a voltage plateau (up to point C3) which is lower than the potential where electrodes that have been deliberately constructed from $Li_2CO_3$ evolve significant $CO_2$ (about 4.3 V).[12] Thus it is primarily $Li_2O_2$ that is being oxidized at this 3.9 V plateau (along with some Li-$RCO_3$ from electrolyte decomposition, as discussed below). Full charge to the equivalent discharge capacity results in removal of $Li_2O_2$ to produce a relatively clean carbon surface, although residuals remain (Figure S4). Analysis of the decomposition products in the electrodes by ToFSIMS at the points indicated by D→C3 are summarized in Figure 4, and selected ToFSIMS spectral images are shown in Figure S5. The normalized

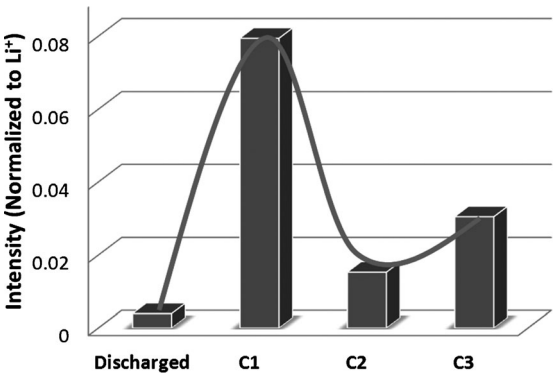


***Figure 4.*** ToFSIMS intensity (normalized to $Li^+$) for the characteristic carbonate positive ion fragment ($Li_3CO_3^+$ at $m/z = 81$) in spectra that probe the electrodes at the points on discharge and charge shown in Figure 3.

intensity of the secondary-ion $Li_3CO_3^+$ fragment (mass = 81, normalized to $Li^+$) is shown as a function of the cycle stage. This fragment is highly characteristic for alkali carbonates,[13] as also shown by our own data for $Li_2CO_3$ (see the Supporting Information). The spectra demonstrate that little carbonate is deposited on discharge, in agreement with our previous finding that TEGDME is "relatively" stable to superoxide attack. However, on the initial charge step to C1, a dramatic thirty-fold increase in the carbonate content on the electrode indicates that electrolyte decomposition commences almost immediately. The normalized intensity of the $Li_3CO_3^+$ fragment is essentially the same as the intensity observed for pure $Li_2CO_3$ (see Table S1 in the Supporting Information). We see a similar trend for the negative ion spectra characterized by the $LiCO_3^-$ fragment (mass = 67; intensity normalized to $O^{2-}$; Figure S6). The reactivity we observe is in full accord with the findings of McCloskey et. al, who observed $CO_2$ evolution on charge through differential electrochemical mass spectroscopy (DEMS), indicating that $Li_2O_2$ reacts with both the carbon surface and the electrolyte to produce a layer of $Li_2CO_3$.[14] The $Co_3O_4$/RGO electrode may moderate that reactivity. Note that DEMS probes the evolved gases as a function of oxidation (regardless of when the carbonates are formed in the cycle), whereas ToFSIMS probes the first few nanometers of the solid interface itself.

The reaction of the electrolyte with liberated oxygen must also be considered. Whether peroxide oxidation proceeds through a direct $2e^-$ oxidation: $< Li_2O_2 \rightarrow O_2 + 2Li^+ + 2e^- >$, or a two-step oxidation: $< Li_2O_2 \rightarrow LiO_2 + Li^+ + e^-$; $LiO_2 \rightarrow Li^+ + e^- + O_2 >$ the nascent $O_2$ that is released at the surface of the $Li_2O_2$ nanocrystallites could also readily react with the electrolyte. As has been pointed out by Armand et al.,[17] the oxidation of $H_2O_2$ results in highly reactive singlet $O_2$ ($^1\Delta_g$) as an excited state with a lifetime ranging from seconds to microseconds;[16] the oxidation of $Li_2O_2$ may similarly produce singlet oxygen. Singlet oxygen is also produced by the

dismutation of superoxide ($2\,HO_2^{\bullet} \rightarrow H_2O_2 + {}^1O_2$).[17] This species is 0.98 eV higher in energy than the ground-state triplet $O_2$ and its reactivity with organic compounds is well-established. Whether or not singlet oxygen is the reason here, the TOFSIMS spectra at point C1 show that the organic lithium carbonates that are formed through reaction of the peroxide and/or released oxygen with the electrolyte deposited on the surface of the lithium peroxide nanocrystallites. Sudden loss of the peroxide interfacial interaction would explain the disintegration of the toroidal aggregate structure, coincident with the onset of oxidation as observed. This is why we believe the initial reaction on oxidation involves nascent evolved oxygen ($*O_2$) in solution rather than peroxide interaction with the carbon surface. The latter would be unlikely to collapse the toroidal structure, whereas $*O_2$ would form at every $Li_2O_2$ nanocrystal surface within the aggregate.

The carbonate residuals have an important effect on cycling which is mediated by the presence of $Co_3O_4$/RGO. Poor capacity retention on cycling can result from clogging of the porous membrane with $Li_2O_2$, and corrosion of the negative metallic Li electrode.[4] To minimize these effects, and allow us to more easily probe the effect of the metal oxide promoter, the discharge capacity of both Li-$O_2$ cells was limited to 6000 mAh $g_C^{-1}$ (about $^1/_2$ of the full capacity). The $Co_3O_4$/RGO/KB electrode achieved a charge of 6000 mAh $g_C^{-1}$ for over seven cycles (Figure 5a) but the KB electrode displayed a poorer rechargeability and sharp capacity fading. This was also evident at limit of 2000 mAh $g_C^{-1}$ as shown in Figure 5b. The $Co_3O_4$/RGO promoter has a strongly favorable effect, namely by increasing the capacity retention by about 25%.

The reason that cycling does not persist is revealed by the discharge–charge profiles shown in Figure 5c, and the SEM images shown in Figure 5d–f. When a charge voltage cut-off of 4.25 V is imposed on the first cycle, full reversible capacity is only maintained for the first few cycles (Figure 5b). Full capacity on charge is not attained on subsequent cycles. Furthermore, the reduction of the OE overpotential effected by the $Co_3O_4$/GO and a distinct charge plateau, is only present on the first charge (Figure 5c). SEM was used to examine the product formed after the 1st, 3rd, and 18th discharge (Figure 5d, e, and f, respectively). Figure 5d shows that well-defined toroids are clearly in abundance after the first discharge to 2000 mAh $g_C^{-1}$. Compared to a discharge capacity of 6000 mAh $g_C^{-1}$ shown previously, these toroids are smaller in thickness and cover less of the surface. Toroids are also evident for an electrode that has been cycled twice and then stopped at a 2000 mAh $g_C^{-1}$ discharge (Figure 5e). While their morphology is similar to the first discharge, they are accompanied by a film that covers the electrode surface. Upon further cycling to the same cut-off capacity on the 18th discharge, vestigial $Li_2O_2$ toroids are barely visible and the film now dominates the electrode surface. These findings are in concert with reports that cycling in TEGDME to maximum discharge results in the disappearance of $Li_2O_2$ from the XRD pattern after five cycles.[18]

An overall picture of the Li-$O_2$ cell on cycling, and the effect of $Co_3O_4$/RGO can thus be proposed as follows. Oxygen reduction catalyzed at the carbon surface produces

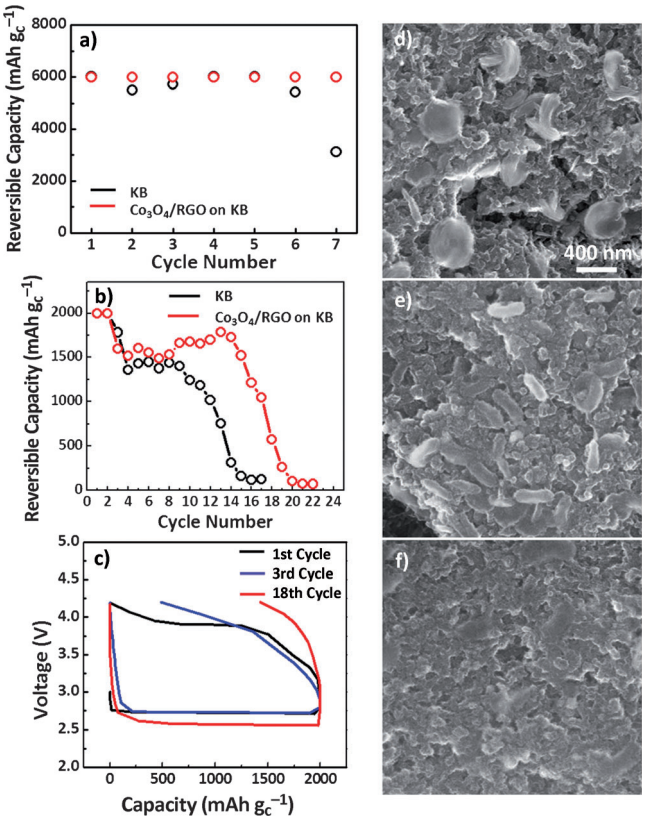


***Figure 5.*** a) Cycling performance of KB and $Co_3O_4$/RGO/KB electrodes (discharge cut-off 6000 mAh $g_C^{-1}$, upper voltage cutoff 4.3 V). b) Cycling performance of KB and $Co_3O_4$/RGO/KB electrodes (discharge cut-off 2000 mAh $g_C^{-1}$, upper voltage cutoff 4.3 V). c) Charge/discharge curves for the $Co_3O_4$/RGO/KB electrode at different stages of cycling shown in (b). SEM micrographs of the discharged electrode after the d) 1st cycle, e) 3rd cycle, and f) 18th cycle, corresponding to the charge/discharge curves shown in (c).

superoxide, whose surface mobility is promoted by the presence of $Co_3O_4$/RGO, thus enhancing the kinetics of formation of $Li_2O_2$. At the immediate onset of the subsequent charge cycle at about 3.3 V, reaction of the electrolyte with peroxide—or much more likely with the nascent $O_2$ that it evolves on oxidation—deposits organic carbonates on the nanocrystalline peroxide surface. Disintegration of the toroidal aggregates and loss of peroxide crystallinity results in collapse of the peroxide/carbonate to form a layer that coats the carbon surface. The $Co_3O_4$/RGO electrode may aid in lowering the OE voltage by either facilitating the mobility of $Li_xO_2$ species released on oxidation, and/or by decreasing the reactivity of the nascent $O_2$ that is released (potentially, by catalyzing the conversion of singlet to triplet oxygen and thus lowering the average oxidation potential). On the first cycle, in the presence of $Co_3O_4$/RGO, the oxidation potential remains below 3.8 V, whereas it increases above 4.25 V in its absence. Nonetheless, towards the end of charge, there is a second, albeit smaller, increase in carbonate formation in the ToFSIMS spectra (Figure 4). The increase in $CO_2$ production above 4.3 V observed by others using DEMS analysis is ascribed to oxidation of $Li_2CO_3$ from the carbon surface produced through reaction with $Li_2O_2$.[14] We note that

any $CO_2$ released into solution will react with superoxide produced by OR on the subsequent discharge, to form yet more "inorganic" $Li_2CO_3$.[19] Its deposition further blocks active sites for OR on the carbon surface. Hence, after multiple cycles of the Li-$O_2$ cell, the continuous build-up of carbonates on the cathode surface terminates the cell activity.

In summary, while $Co_3O_4$/RGO clearly enhances the kinetics of mass (or surface) transport for both OR and OE, it does not appear to operate through a conventional electrocatalytic mechanism. On cycling, the significant improvement in transport is overwhelmed by the deposition of side products resulting from parasitic reactions with the electrolyte. Reactivity of liberated $*O_2$ and/or peroxide with the TEGDME electrolyte (and probably with many organic electrolytes) on charge is a far greater challenge than superoxide reactivity on discharge, as our results show. We believe that these findings are broadly applicable to a range of metal oxide catalysts and electrolytes. This understanding should inspire next steps to better understand surface reactivity and tailor electrodes and electrolytes to overcome the limitations.

## Experimental Section

The synthesis of the graphene/$Co_3O_4$ hybrid materials was accomplished through a modification of a previously reported method as described in the Supporting Information.[9] X-ray diffraction of the materials and electrodes was carried out on a Bruker D8-Advance (Cu-Kα radiation). FESEM imaging was performed on a LEO 1530 field-emission SEM. ToF-SIMS spectra were collected on a ToFSIMS4 spectrometer (ION-TOF Gmbh) with 50 keV $Bi_3^{2+}$ primary ions. Mass spectra were obtained in high mass resolution mode from a 500 μm × 500μm imaged region on each sample.

Received: July 7, 2012
Published online: November 19, 2012

**Keywords:** electrocatalysis · electrochemistry · graphene · lithium–oxygen batteries · peroxides

[1] K. M. Abraham, Z. Jiang, *J. Electrochem. Soc.* **1996**, *143*, 1 – 5.
[2] G. Girishkumar, B. McCloskey, A. C. Luntz, S. Swanson, W. Wilcke, *J. Phys. Chem. Lett.* **2010**, *1*, 2193 – 2203.
[3] A. Débart, J. Bao, G. Armstrong, P. G. Bruce, *J. Power Sources* **2007**, *174*, 1177 – 1182.
[4] A. Débart, A. J. Paterson, J. Bao, P. G. Bruce, *Angew. Chem.* **2008**, *120*, 4597 – 4600; *Angew. Chem. Int. Ed.* **2008**, *47*, 4521 – 4524.
[5] Y. C. Lu, Z. Xu, H. A. Gasteiger, S. Chen, K. H. Schifferli, Y. S. Horn, *J. Am. Chem. Soc.* **2010**, *132*, 12170 – 12171.
[6] L. Wang, X. Zhao, Y. Lu, M. Xu, D. Zhang, R. S. Ruoff, K. J. Stevenson, J. B. Goodenough, *J. Electrochem. Soc.* **2011**, *158*, A1379 – A1382.
[7] Y. Liang, Y. Li, H. Wang, J. Zhou, J. Wang, T. Reigier, H. Dai, *Nat. Mater.* **2011**, *10*, 780 – 786.
[8] B. D. McCloskey, R. Scheffler, A. Speidel, D. S. Bethune, R. M. Shelby, A. C. Luntz, *J. Am. Chem. Soc.* **2011**, *133*, 18038 – 18041.
[9] S. Yang, G. Cui, S. Pang, Q. Cao, U. Kolb, X. Feng, J. Maier, K. Mullen, *ChemSusChem* **2010**, *3*, 236 – 239.
[10] J. Xiao, D. Mei, X. Li, W. Xu, D. Wang, G. L. Graff, W. D. Bennett, Z. Nie, L. V. Saraf, I. A. Aksay, J. Liu, J.-G. Zhang, *Nano Lett* **2011**, *11*, 5071 – 5078.
[11] R. Black, S. Oh, J. H. Lee, T. Yim, B. Adams, L. F. Nazar, *J. Am. Chem. Soc.* **2012**, *134*, 2902 – 2905.
[12] R. R. Mitchell, B. M. Gallant, C. V. Thompson, Y. Shao-Horn, *Energy Environ. Sci.* **2011**, *4*, 2952 – 2958.
[13] L. F. Liotta, M. Ousmane, G. DiCarlo, G. Pantaleo, G. Deganello, G. Marci, A. Giroir-Fendler, *Appl. Catal. A* **2008**, *347*, 81 – 88.
[14] B. D. McCloskey, D. S. Bethune, R. M. Shelby, G. Girishkumar, A. C. Luntz, *J. Phys. Chem. Lett.* **2011**, *2*, 1161.
[15] A. D. Shaw, M. M. Cortez, A. K. Gianotto, J. E. Olson, C. Karahan, R. Avci, G. S. Groenewold, *Surf. Interface Anal.* **2003**, *35*, 310 – 317.
[16] B. D. McCloskey, A. Speidel, R. Scheffler, D. C. Miller, V. Viswanathan, J. S. Hummelshoj, J. K. Norskov, A. C. Luntz, *J. Phys. Chem. Lett.* **2012**, *3*, 997 – 1001.
[17] J. Hassoun, F. Croce, M. Armand, B. Scrosati, *Angew. Chem.* **2011**, *123*, 3055 – 3058; *Angew. Chem. Int. Ed.* **2011**, *50*, 2999 – 3002.
[18] M. Kasha, A. U. Khan, *Ann. N. Y. Acad. Sci.* **1970**, *171*, 5 – 23.
[19] E. A. Mayeda, A. J. Bard, *J. Am. Chem. Soc.* **1974**, *96*, 4023.
[20] S. Freunberger, Y. Chen, N. Drewett, L. Hardwick, F. Barde, P. G. Bruce, *Angew. Chem.* **2011**, *123*, 8768 – 8772; *Angew. Chem. Int. Ed.* **2011**, *50*, 8609 – 8613.
[21] K. Takechi, T. Shiga, R. Asaoko, *Chem. Commun.* **2011**, *47*, 3463 – 3465.

  